Non-Boronized Operation of ASDEX Upgrade with Full-Tungsten Plasma Facing Components

A. Kallenbach, R. Dux, M. Mayer, R. Neu, T. Pütterich, V. Bobkov, J.C. Fuchs, T. Eich, O. Gruber, A. Herrmann, L.D. Horton, C.F. Maggi, H. Meister, R. Pugno, V. Rohde, A. Sips, A. Stäbler, J. Stober and ASDEX Upgrade Team

Max-Planck-Institut für Plasmaphysik, EURATOM Association, Garching, GERMANY
e-mail: Arne.Kallenbach@ipp.mpg.de

Abstract After completion of the tungsten coating of all plasma facing components, ASDEX Upgrade has been operated without boronization for 1 1/2 experimental campaigns. This has allowed the study of fuel retention under conditions of relatively low D co-deposition with low-Z impurities as well as the operational space of a full-tungsten device for the unfavourable condition of a relatively high intrinsic impurity level. Restrictions in operation were caused by central accumulation of tungsten in combination with density peaking, resulting in H-L backtransitions induced by too low separatrix power flux. Most important control parameters have been found to be the central heating power, as delivered predominantly by ECRH, and the ELM frequency, most easily controlled by gas puffing. Generally, ELMs exhibit a positive impact, with the effect of impurity flushing out of the pedestal region overbalancing the ELM induced W source. The accumulation of tungsten around the pedestal top is supposed to be connected to the large neoclassical impurity inward pinch caused by the steep density gradients in the edge transport barrier region. ICRF operation suffered from the higher intrinsic low-Z impurity content, causing a large W source due to ICRF induced sheath acceleration. Clearly more favourable conditions were observed after boronization, where the ICRF induced W influx was considerably reduced. The restrictions of plasma operation in the unboronized W machine occured predominantly under low or medium power conditions. In the operation domain above about 60% of the target power load limit ($\approx$ 10 MW/m^2), stable operation with virtually no difference between boronized and unboronized discharges was achieved.

1. Introduction

With the 2007 experimental campaign, the ASDEX Upgrade tokamak completed its conversion into a device with 100 % tungsten plasma facing components (PFCs) [1]. In order not to compromise the results obtained for plasma operation in a high-Z device, no boronization was performed before startup and during the first 1 1/2 experimental campaigns. Old boron layers had been mechanically removed during the preceding vent as much as possible. Operation with no carbon tiles facing directly the plasma and without boronization allowed the study of fuel retention with low levels of fuel co-deposition with B and C. On the other hand, the relatively high impurity level in the unboronized machine lead to restrictions of the H-mode operational space, since low-medium Z impurities dominate the physical sputtering of tungsten. In particular, ICRF heated discharges suffered from large radiative losses due to tungsten sputtered by impurities accelerated in sheath-rectified electric fields at the antenna limiters.

2. Campaign integrated deposited layers and fuel retention

Post-campaign analysis of C and B layers on PFC surfaces as well as D retention measurements allowed the characterisation of fuel retention over the C $\rightarrow$ W PFC transition [2] [3]. Figure 1 shows a large reduction of C deposition in the inner divertor after W coating of the outer limiters, identifying these limiters as a dominant C source. The corresponding D codeposition exhibited a less pronounced reduction as expected from the C reduction due to the remaining D codeposition with B. The latter almost vanished after cleaning of the PFCs and non-boronized all-W operation. For these conditions, D retention in the outer divertor due to deep diffusion and trapping in W becomes an important retention mechanism, albeit at a much lower absolute level compared to a low-Z PFC device. The long term D retention in the full-W device from

surface analysis was found to be 0.4 - 0.6 % of the gas input [2]. Compared to the post-mortem analysis, higher values of retained D have been observed by short term in situ gas balance measurements (3.6 $\pm$ 2.7 % for an H-mode with gas puff) [4]. The difference is explained by the medium and long term release of D, a larger uncertainty of the gas balance measurements has to be considered.

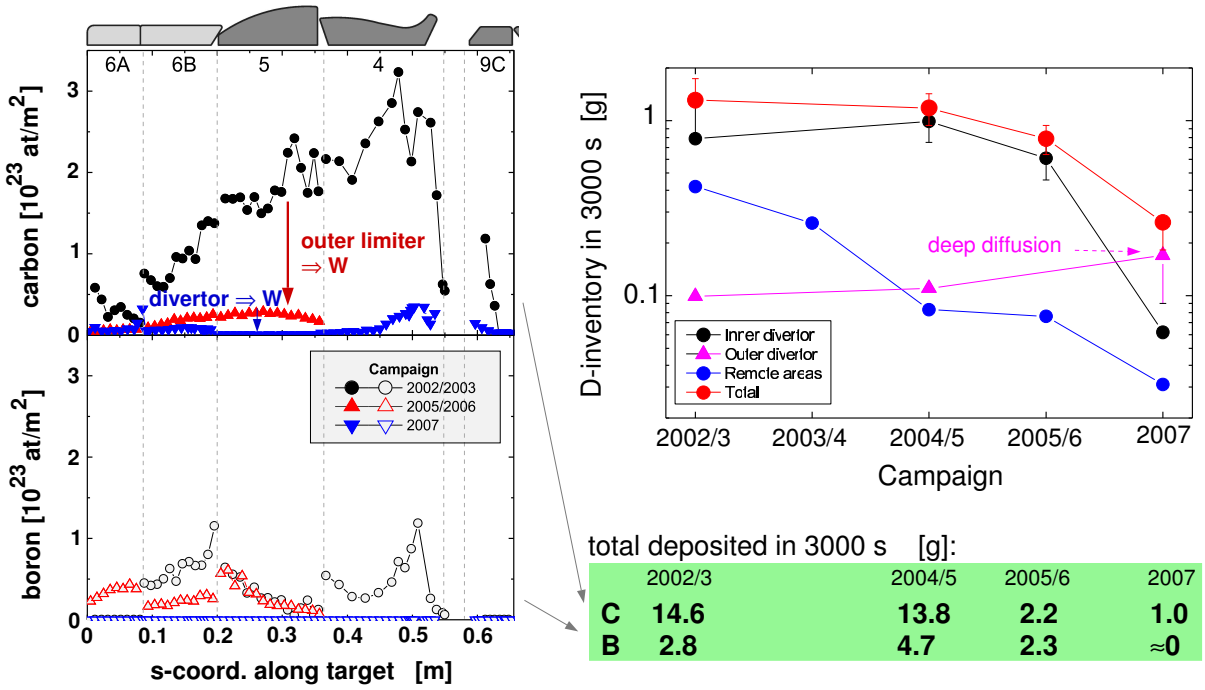

Figure 1: *Deposited C and B layer densities in the inner divertor during the transition from C to W. In 2002/3, the inner heat shield and upper inner divertor were W coated, the coating of the lower divertor before the 2007 campaign completed the transformation to full-W. Also shown is the temporal evolution of the D content for various plasma facing components. The table gives the total amount of deposited C and B in the inner divertor.*

3. Impact of boronization

The impurity content pre- and post-boronization has been monitored by various spectroscopic systems. Figure 2 shows the temporal development of the most important intrinsic impurities C, O and F. Boron is hardly detectable before the boronization, CXRS measurements after boronization result in a typical B concentration at the pedestal top of 0.8 %, which slowly decays to 0.4 % over 200 discharges. Despite considerable scatter in the impurity concentrations, the reduction of the O and C levels by the boronization is clearly visible. C experiences a strong reduction, but returns to about half the pre-boronization level after about 30-40 discharges. The general reduction of the C content was in fact less than originally expected for the full-W coating. Remaining sources, with unknown relative contributions, are arc traces cutting through the 4 μm W coating at the inner divertor baffle, photo-desorption from remote surfaces and the release of carbon from uncoated tile sides. Residual gas analysis suggests also the importance of erosion of C by oxygen due to CO and CO_2 formation in the unboronised device. The recycling nature of carbon due to chemical erosion is supposed to explain the resilience of the core C concentration against the reduction of the primary sources [5], which is obvious from the pronounced reduction found in the inner divertor C deposition as shown in figure 1. Many 'outliers' in the concentration plots can in fact be explained by special experimental conditions. E.g., ex-

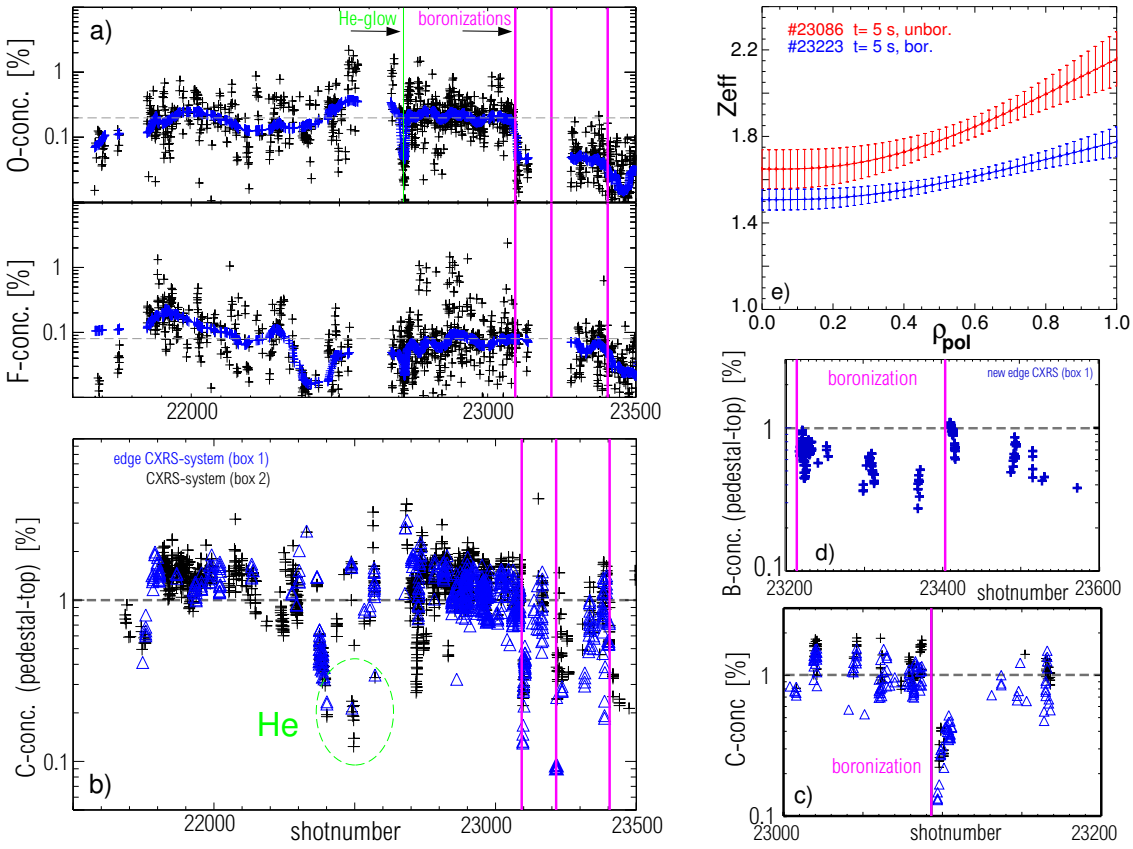

Figure 2: *Development of impurity concentrations during the unboronized, full-W campaign and after boronization. a) O and F concentrations from X-ray lines measured by a Bragg crystal spectrometer ($n_e > 4.5\ 10^{19}\ m^{-3}$). b) C concentrations around the pedestal top measured by the core and edge CXRS systems ($n_e > 4\ 10^{19}\ m^{-3}$, $P_{heat} > 4.5$ MW, $W_{MHD} > 0.3$ MJ). c) expanded view of b) around the first boronization d) boron concentrations from CXRS after boronization e) Z_{eff} profiles from bremsstrahlung for two high power improved H-mode discharges before and after boronization.*

periments investigating the degradation of plasma confinement by elevated helium content [6] also showed reduced impurity concentrations. Radial profiles of Z_{eff} from bremsstrahlung are shown in figure 2e for representative high-power, improved H-mode discharges before and after the first boronization. Z_{eff} is quite well reconciled by the spectroscopic measurements if the contribution of the individual impurities is summed up.

4. Limitations of operational space

The operational space of a full-W device is reduced in comparison to an all-carbon machine. Dedicated experiments were performed to map the operational space of the unboronized device, to understand the mechanisms leading to limitation of the operational space and to document its recovery after boronization.

4.1. Central radiation limit due to W accumulation An important limit for H-mode operation with tungsten PFCs is excessive central radiation due to tungsten accumulation close to the magnetic axis. Figure 3 shows a typical example for tungsten accumulation in combination with central density peaking. The accumulation limit is a consequence of the tungsten source, the impurity removal from the pedestal region by ELMs and the central power balance, which determines the anomalous transport level in the center. Important experimental actuators are

ECRH heating (central power balance) and D_2 gas puffing (ELM frequency, no pellet pacemaking was available in the 2007 / early 2008 campaigns). Dedicated experiments with variations of the central heating power and gas flux resulted in a comprehensive experimental characterisation of the W accumulation limit. Figure 4 shows 4 discharges with different combinations of central ECRH and gas puffing at the edge of the stable operational domain. 2 discharges with sufficient central ECRH and gas puff are stable, while the discharges with the lowest gas puff and the lowest ECRH power showed central density peaking in combination with W accumulation. A runaway situation is obtained when the tungsten radiation in the plasma center approaches a considerable fraction of the heating power flow. Under these conditions, the

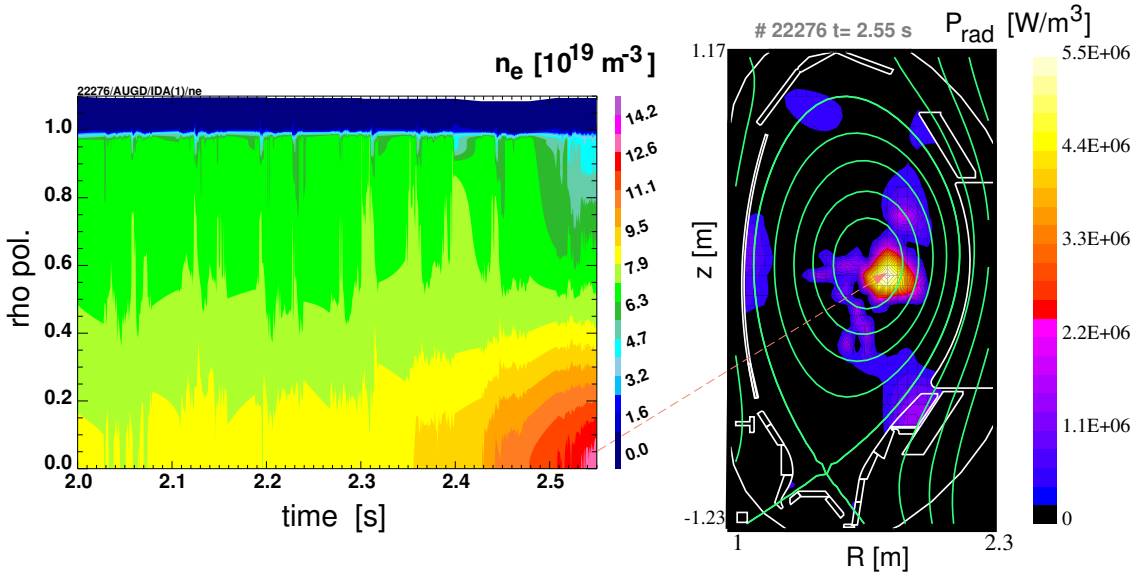

Figure 3: *Density profile evolution and reconstructed radiated power distribution for a discharge with central density peaking and tungsten accumulation due to insufficient central heating and/or gas puffing, see figure 4.*

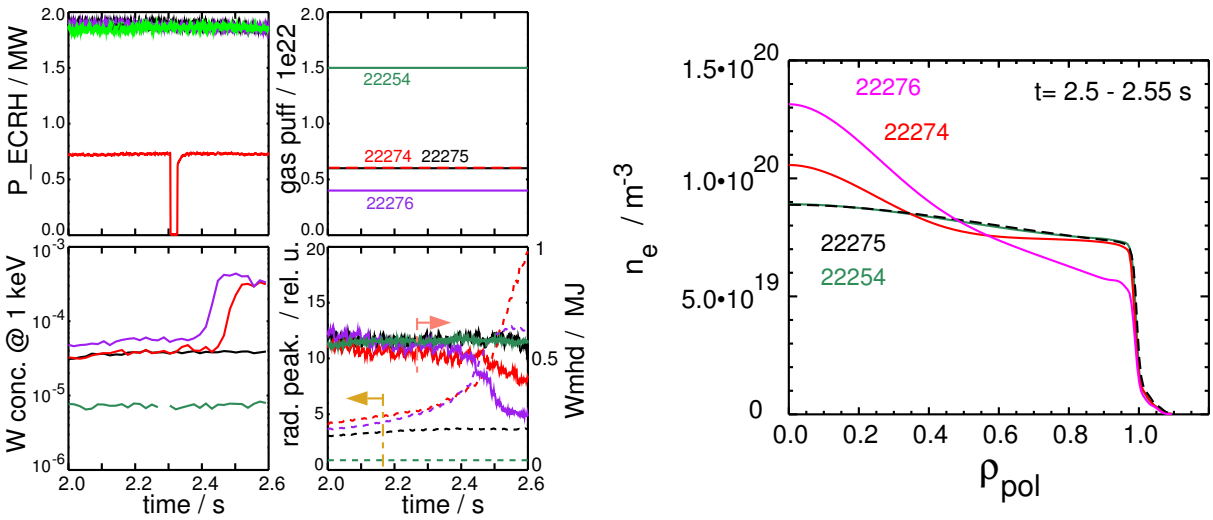

Figure 4: *Time traces and density profiles of 4 discharges with different levels of central ECRH heating and gas puff. Cases with too low gas puff or ECRH power exhibit density peaking, central W accumulation and finally an H-L transition.* P_{NBI}*= 5 MW,* I_p*= 1 MA.*

anomalous transport is reduced, and the (deuteron) density profile peaks. The peaking leads to an increased neoclassical inward flux of tungsten, leading to increasing radiated power. Finally, the conducted power flow becomes too low to sustain the H-mode, and a H-L transition occurs. Usually, after an L-mode phase most of the tungsten is lost from the core and the discharge re-enters the H-mode. For low enough tungsten concentrations, stable central peaking of tungsten is also observed, which is possible as long as the central power balance is not disturbed too much. Scans of the ECRH deposition radius revealed that a very central deposition (inside $\rho_{pol} = 0.2$) is essential to prevent density peaking.

4.2. Operational space of full-W ASDEX Upgrade with and without boronization Figure 5 shows the operational space of full-W AUG in terms of neutral gas flux and power flow to the divertor target, expressed by the difference of heating power and total radiated power. The upper limit of P_{heat}-P_{rad} is a machine limit and corresponds to a time-averaged power density at the outer divertor of about 10 MW/m^2. This limit increases slightly with the neutral gas level due to the broadening of the target power load profile with density / neutral flux [7]. The lower limit for P_{heat}-P_{rad} can be the H-L power threshold, but here the W accumulation limit is more important, since the low type-I ELM frequency at small separatrix power flows produces an experimental situation prone to W accumulation. At high values of the divertor neutral flux and low power, the type-III ELMy regime is located. Here, density peaking and W accumulation are observed also at high (type-III) ELM frequencies. However, due to the reduced confinement (typically H_{98y2} below 0.9), this regime is not of primary interest. Of particular importance are

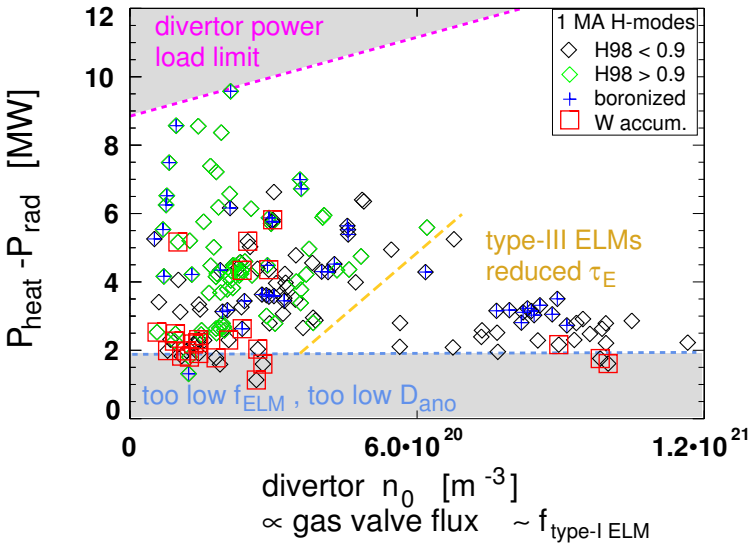

Figure 5: *H-mode operational space in terms of divertor neutral flux and target heat load, P_{heat}-P_{rad}. Data points represent either steady state flattop phases or phases leading to central W accumulation (red squares), averaging time is typically 0.5 s. The divertor neutral density, $n_{0,div}$, is nearly proportional to the total gas valve flux. Black diamonds denote discharges with H-factors H_{98y2} below 0.9, which are typically type-III [8]. The limits indicated are just sketches guided by the data points. Plasma current I_p= 1 MA.*

the discharges with W accumulation at higher values of P_{heat}-P_{rad}. With one exception, these discharges were run without boronization. The W accumulation is supposed to be caused by insufficient central heating power in view of the actual impurity content. In the high power operational domain, there is a wide window below the maximum power flux where stable operation is achieved and no influence of the boronization state is observed. More information

about the operational space and relevant plasma parameters of the discharges shown in figure 5 are given in figure 6. For the predominantly type-I ELMy discharges without boronization, an ELM frequency above 100 Hz is required for stable operation. Analogously, a corresponding high neutral density or gas puff rate is required. On the right figure 6, it is clearly shown that the central radiation strongly correlates with the tungsten concentration. Quantitative analysis shows that for the high radiation levels, tungsten radiation dominates the radiative losses [9].

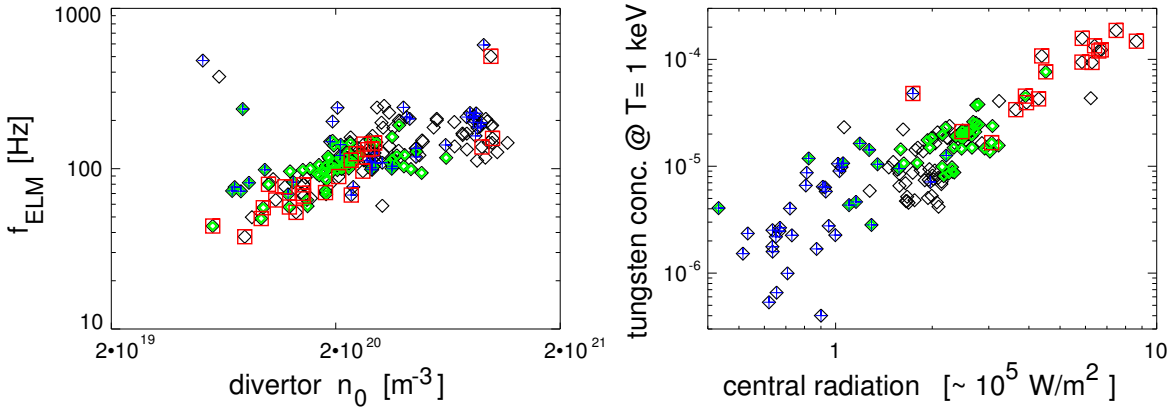

Figure 6: *ELM frequency versus divertor neutral density (left) and tungsten concentration derived from the W quasicontinuum emitting around T_e= 1 keV versus line integrated radiation from a central bolometer chord(right), same data points and symbols as in figure 5. Note that during W accumulation, the quasicontinuum emission region broadens and shifts inward.*

5. Tungsten source distribution and contribution to core W content

To improve operation of a full-W tokamak, and to overcome as far as possible the negative impact of strong W sources, knowledge about the spatial distribution of the sources and their relative impact on central impurity concentration is essential. Detailed spectroscopic analysis of the tungsten source distribution revealed considerable variations of source strengths and their impact on core W concentration [10]. The strongest W source is the outer divertor, but it has a small contribution to the core W content. Inner wall and outer limiters supply about similar W influxes, depending on the relative inner and outer wall gaps (see figure 7 for variation of distance to outer limiters). A significant fraction of the W source on all PFCs is caused by ELMs, with a higher relative contribution at lower inter-ELM edge temperatures. The core W content is usually dominated by the LFS limiter W source. The large penetration probability for W sputtered on the outer limiters poses a problem to ICRF operation in an all-W device. W sputtered by sheath rectified voltages caused predominantly by antenna box currents [11] [12] can lead to central W radiation comparable to the absorbed ICRF power for unboronized conditions. After the boronization, more favourable conditions with $P_{ICRH}/\Delta P_{rad,ICRH}$ = 3 have been obtained, even after the boron coating has been eroded from the limiters.

Despite the significant contribution of ELMs to the sputtered W flux, increasing the ELM frequency always leads to a reduction of the W content due to the flushing of the impurities out of the pedestal region. This is demonstrated in figure 7. The line integrated SXR intensity shown for the shots with lowest and highest ELM frequency on the r.h.s of figure 7 shows clearly the pronounced impurity rise in between ELMs around the pedestal top. Although the stronger low-frequency ELMs produce a larger drop in the SXR emission, a step-wise rise of the emission level occurs. Comparing the rise in SXR emission at the pedestal top for the different ELM frequencies, a similar rise rate is observed after the ELM crash. This similar rise rate suggests that in fact the impurity transport is responsible for the rise in core W content. A possible screening

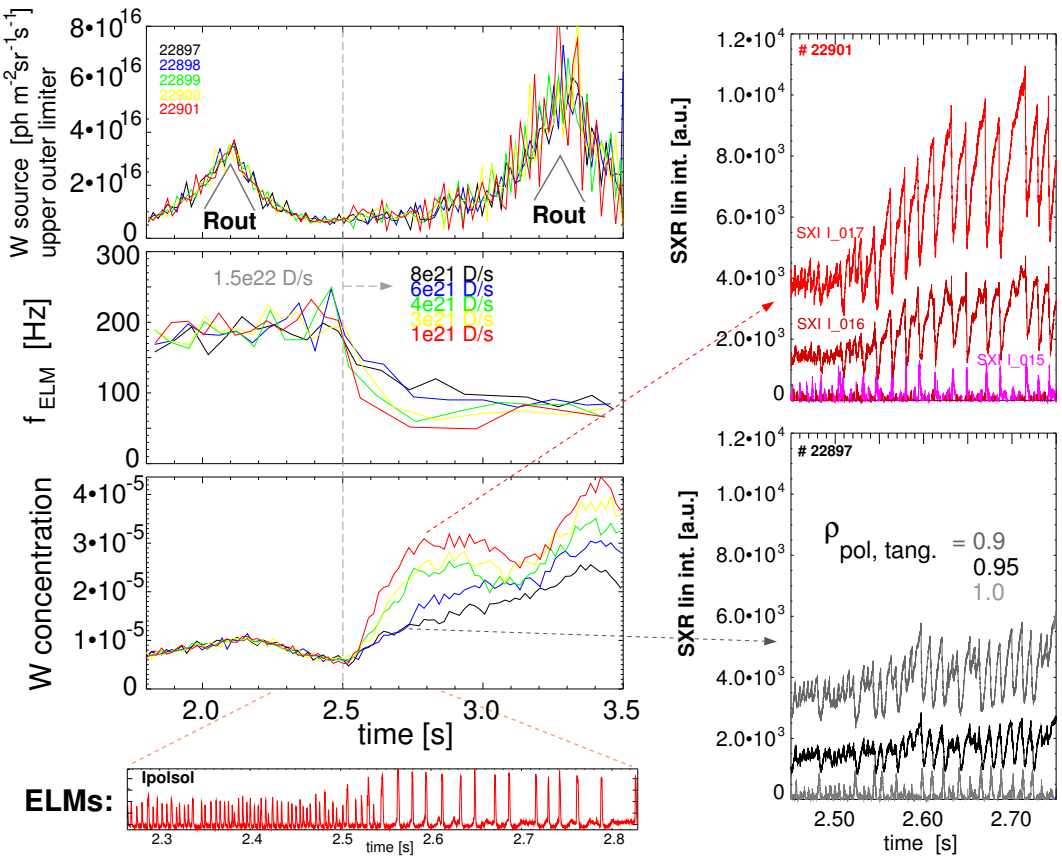

Figure 7: *Variation of core W concentration @ $T_e \approx 1$ keV with ELM frequency. f_{ELM} has been varied by reducing the gas puff to different values. The tungsten source, as measured at the upper part of the outer limiter, remains constant over the change of f_{ELM}. An increase of the source is observed during an outward shift of the plasma column (Rout $\bigwedge$) closer towards the limiters. P_{heat} is 6.5 MW before t=2.8 s and 9 MW afterwards, P_{rad} rises from 3.5 to 4.5 MW with the additional NBI source switched on a t= 2.8 s. On the r.h.s., the line integrated SXR emission is shown for 3 edge channels with tangency radii of ρ_{pol}=0.9, 0.95 and 1.*

of W in the SOL plasma due to the higher edge density caused by the higher gas puff appears to be less important. The strong sensitivity of the core tungsten content on the ELM frequency is thought to be connected to the strong neoclassical inward pinch over the steep density gradient in the edge transport barrier region [13]. Since the particle loss per ELM rises with reduced type-I ELM frequency [7], transport effects are thought to contribute to the almost inverse relation of ELM frequency and tungsten concentration for the conditions of figure 7. Tungsten ions accumulated at the pedestal top have more time to diffuse further into the core at reduced ELM frequency.

6. Conclusions

Operation of a full-metal device without boronization is the only way to study fuel retention under conditions of very small co-deposition. In fact, the codeposition of D with low-Z impurities in AUG could be reduced so far that deep trapping of hydrogen in the bulk material becomes a relevant long-term storage mechanism, with retention rates well below a percent of the gas input. In-situ gas balance measurements revealed ceasing fuel storage of D after an initial discharge phase with a dynamic wall retention corresponding to about 50 monolayers [14]. Since sputtering by low- and medium-Z impurities dominates the erosion of tungsten, the H-mode

operational window in terms of mimimum required values of gas puffing and central heating is somewhat reduced comparing un-boronized with boronized operation. The operational limit is set by the occurrence of central tungsten accumulation and central radiative losses comparable to the local heating. The limit is understood as a consequence of the tungsten source, predominantly at the low field side limiters, the frequency and size of ELMs flushing the tungsten ions out of the pedestal region and the central anomalous transport level which counteracts the neoclassical inward drifts. A higher impurity level may increase or decrease the tungsten source, depending on the counteracting effects of increased impurity fluxes and reduced edge temperatures. However, impurities lead always to a reduced ELM frequency due to radiative power removal inside the separatrix.

The reduction of the operational space in an un-boronized machine disappears if the divertor power load becomes the limiting quantity. In this case, seed impurities have to be added to the plasma for radiative power exhaust. While seed impurities produce competing effects with regard to the tungsten source (high impurity flux to the wall, but reduced edge temperature and impact energy), the reduction of ELM frequency caused by the additional radiation leads to less favourable impurity transport. Due to the strong neoclassical inward drift for tungsten in the edge transport barrier region, a more sensitive dependence for W is expected compared to low-Z impurities. Therefore, a reliable control of the ELM frequency at sufficiently high level is mandatory for full-tungsten operation with high radiation level. In addition to the pellet approach, ELM control by resonant magnetic perturbations is expected to become an important tool in combination with full tungsten plasma facing components. Helpful for successful operation is also a high fraction of central heating power. Modifications of the ICRF antennas are under development [15], which are expected to significantly reduce the tungsten sputtering rate at the end of field lines crossing the antenna boxes.

References

[1] NEU, R. et al., Plasma Phys. Controlled Fusion **49** (2007) B59.
[2] MAYER, M. et al., Nucl. Fusion **47** (2007) 1607.
[3] MAYER, M. et al., Carbon balance and deuterium inventory from a carbon dominated to a full tungsten ASDEX Upgrade, PSI 2008 conference, subm. to Journ. Nucl. Mat.
[4] ROHDE, V. et al., Gas balance in ASDEX Upgrade with tungsten first wall, PSI 2008 conference, subm. to Journ. Nucl. Mat.
[5] KALLENBACH, A. et al., J. Nucl. Mater. **363-365** (2007) 60.
[6] NEU, R. et al., Influence of the ^{4}He concentration on H-mode confinement and transport in ASDEX Upgrade, in *Europhysics Conference Abstracts (CD-ROM, Proc. of the 35rd EPS Conference on Plasma Physics, Hersonissos, Crete, 2008)*, volume 32F, pages P–4.039, Geneva, 2008, EPS.
[7] KALLENBACH, A. et al., Nucl. Fusion **48** (2008) 085008.
[8] RYTER, F. et al., Journal of Physics: Conference Series **123** (2008) 012035.
[9] KALLENBACH, A. et al., Plasma Phys. Controlled Fusion **47** (2005) B207.
[10] DUX, R. et al., Plasma-wall interaction and plasma behaviour in the non-boronised all tungsten in ASDEX Upgrade, PSI 2008 conference, subm. to Journ. Nucl. Mat.
[11] COLAS, L. et al., Plasma Phys. Controlled Fusion **49** (2007) B35.
[12] BOBKOV, V. et al., Operation of ICRF antennas in a full tungsten environment in ASDEX Upgrade, PSI 2008 conference, subm. to Journ. Nucl. Mat.
[13] PÜTTERICH, T. et al., Fast CXRS-measurements in the edge transport barrier of ASDEX Upgrade, in *Europhysics Conference Abstracts (CD-ROM, Proc. of the 35rd EPS Conference on Plasma Physics, Hersonissos, Crete, 2008)*, volume 32F, pages P–2.083, Geneva, 2008, EPS.
[14] ROHDE, V. et al., this conference (2008).
[15] BOBKOV, V. et al., Calculations of near-fields of icrf antenna for ASDEX Upgrade, in *Europhysics Conference Abstracts (CD-ROM, Proc. of the 35rd EPS Conference on Plasma Physics, Hersonissos, Crete, 2008)*, volume 32F, pages P–5.005, Geneva, 2008, EPS.